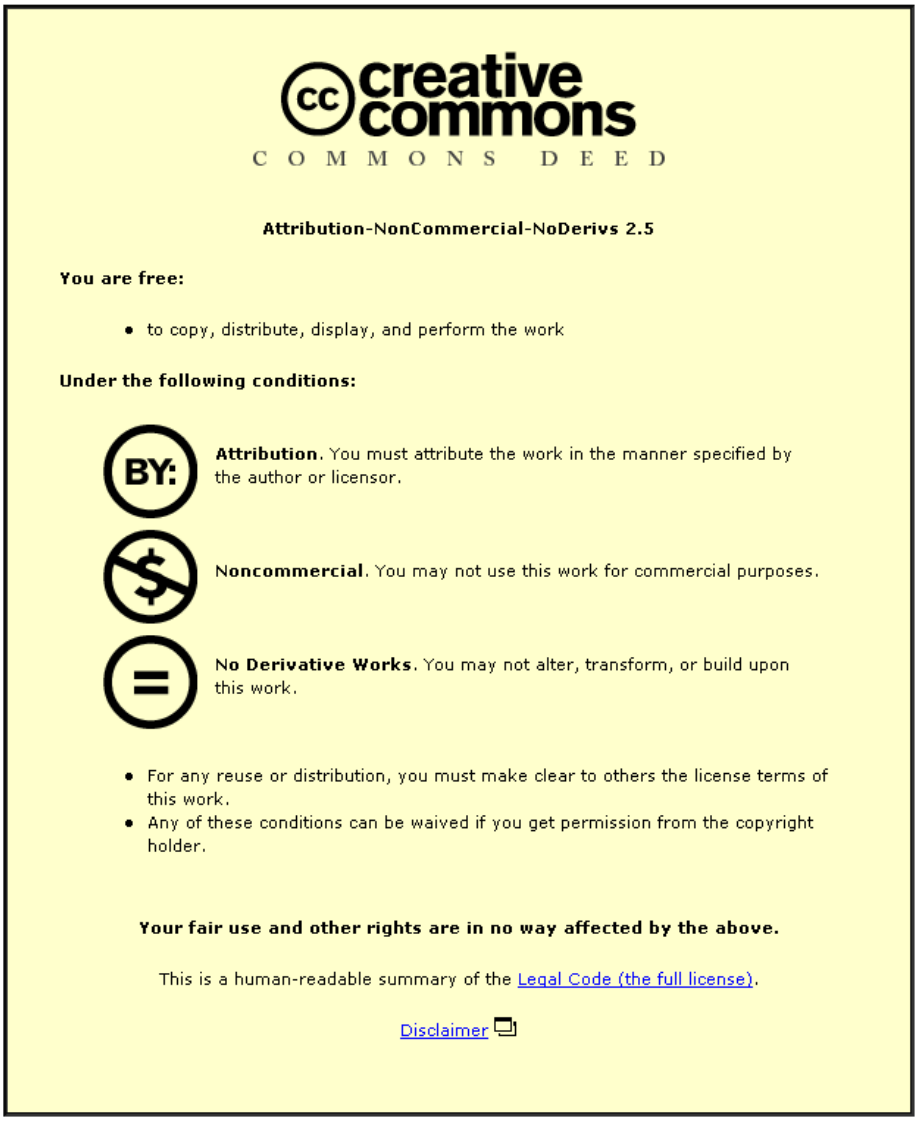

creative commons

COMMONS DEED

Attribution-NonCommercial-NoDerivs 2.5

You are free:

- to copy, distribute, display, and perform the work

Under the following conditions:

Attribution. You must attribute the work in the manner specified by the author or licensor.

Noncommercial. You may not use this work for commercial purposes.

No Derivative Works. You may not alter, transform, or build upon this work.

- For any reuse or distribution, you must make clear to others the license terms of this work.
- Any of these conditions can be waived if you get permission from the copyright holder.

Your fair use and other rights are in no way affected by the above.

This is a human-readable summary of the Legal Code (the full license).

Disclaimer

Exploring Assumptions and Requirements for Continuous Modification of Vehicle Handling using Nonlinear Optimal Control and a New Exponential Tyre Model

Matthew C Best
Dept of Aeronautical and Automotive Engineering
Loughborough University

Ashby Road, Loughborough, Leicestershire, LE11 3TU, UK
Tel: (+44) 1509 227209 Fax: (+44) 1509 227275
E-mail : m.c.best@lboro.ac.uk

An iterative simulation-based nonlinear optimisation technique is used here to explore optimally controlled behaviour of a large RWD vehicle with rear steer and idealised differential actuators. A novel tyre model is also introduced, which uses simple analytic functions for separated calculation of lateral and longitudinal force, with both based on the combined slip and vertical load. By first considering suitable transient and steady-state targets for the yaw rate, optimal control is simulated which is effective throughout the lateral acceleration range. Interestingly this can be closely emulated under stable conditions using PID control of rear steer only, according to the yaw rate target and without the need for separate lateral velocity control. PID is no longer successful when stabilising control is considered, so future research will consider an extension to the nonlinear optimisation method for such cases.

Topics / Vehicle Control, Tyre Property, Integrated Motion Control

1. INTRODUCTION

There is often a fundamental difference between handling controllers that have been developed on production vehicles (eg Bosch ESP [1], and [2]) and recent simulation research on handling control, [3–5]. The former concentrate on interventionist strategies which stabilise the vehicle in extreme situations and generally leave the dynamics unchanged at lower lateral accelerations. The latter (particularly when steer-by-wire and electric / hybrid powertrain actuators are examined) consider control which is 'always on' and alters the vehicle response throughout the acceleration range, often to emulate a reference vehicle.

Two common disadvantages with these latter approaches are that i) improvements at low / mid range acceleration is not considered alongside stabilisation at the limit, and ii) reference vehicles are usually just alternative passive configurations, often using the linear bicycle model. This paper seeks to explore the transition in control from low to high lateral acceleration. The techniques can also be applied to design a continuous nonlinear feedback law from measurable vehicle states (though not within this paper).

The Generalised Optimal Control (GOC) method (seen previously in [6] and [8]) is summarised in Section 2. This is capable of establishing the optimal time history of controls for any given simulation of a smooth (continuously differentiable) nonlinear system. It is a computationally expensive process, requiring repeated re-simulation as the sequence converges, so the results of complementary research into a new tyre model are also presented here, in Section 4. The new tyre model uses a separate set of simple analytic functions for lateral and longitudinal force; this makes the derivative functions simpler, allowing faster optimisation with GOC.

After considering yaw rate targets and desired transient response (Section 5) the GOC sequence is compared with a simple PID controller. To determine the best possible control, GOC is allowed both rear steer and actuation of an idealised differential at the driven rear wheels, whereas the PID control uses rear steer alone. Given the very different scope and nature of derivation of the two control sequences, the performance of the PID controller is surprisingly good, up to the limit of stability.

2. GENERALISED OPTIMAL CONTROL (GOC)

The control optimisation is a nonlinear formulation of LQR; controls are sought to minimise a Hamiltonian which is prescribed in terms of a (nonlinear) system of costate equations over a fixed time period. Given a cost function of time, L and a residual cost associated with final states, L_T :

$$J = L_T\left[\mathbf{x}(T)\right] + \int_0^T L\left[\mathbf{x}(t), \mathbf{u}(t)\right] dt \qquad (1)$$

Adding constraint equations to this with a vector of Lagrange multiplier functions, $\mathbf{p}(t)$:

$$J = L_T\left[\mathbf{x}(T)\right] + \int_0^T \left\{ L\left[\mathbf{x}(t),\mathbf{u}(t)\right] + \mathbf{p}^T(t)\left[g\left[\mathbf{x}(t),\mathbf{u}(t)\right] - \dot{\mathbf{x}}(t)\right]\right\} dt \tag{2}$$

where g is given by the system equations, $\dot{\mathbf{x}} = g\left[\mathbf{x}(t),\mathbf{u}(t)\right]$. The Lagrange multipliers can be formed as a so-called costate system, and the Hamiltonian function can then be defined (see for example [7]) as

$$H = L\left[\mathbf{x}(t),\mathbf{u}(t)\right] + \mathbf{p}^T(t)g\left[\mathbf{x}(t),\mathbf{u}(t)\right] \tag{3}$$

Eqn. 2 can now be integrated by parts to give,

$$J = L_T\left[\mathbf{x}(T)\right] + \mathbf{p}^T(0)\mathbf{x}(0) - \mathbf{p}^T(T)\mathbf{x}(T) + \int_0^T \left\{ H + \dot{\mathbf{p}}^T(t)\mathbf{x}(t)\right\} dt \tag{4}$$

Considering small changes δJ in the dynamic cost caused by small changes in the controls $\delta\boldsymbol{u}(t)$ and in the states $\delta\boldsymbol{x}(t)$:

$$\delta J = \left[\frac{\partial L_T}{\partial \mathbf{x}} - \mathbf{p}^T(T)\right]\delta\mathbf{x}(T) + \mathbf{p}^T(0)\delta\mathbf{x}(0) + \int_0^T \left\{ \left[\frac{\partial H}{\partial \mathbf{x}} + \dot{\mathbf{p}}^T(t)\right]\delta\mathbf{x}(t) + \frac{\partial H}{\partial \mathbf{u}}\delta\mathbf{u}(t)\right\} dt \tag{5}$$

Costates can then be chosen such that δJ depends only on changes in the controls by imposing the following conditions :

$$\dot{\mathbf{p}}^T(t) = -\frac{\partial H}{\partial \mathbf{x}} = -\frac{\partial L}{\partial \mathbf{x}} - \mathbf{p}^T\frac{\partial g}{\partial \mathbf{x}}, \qquad \mathbf{p}^T(T) = \frac{\partial L_T}{\partial \mathbf{x}} \tag{6}$$

$$\text{hence,} \qquad \delta J = \mathbf{p}^T(0)\delta\mathbf{x}(0) + \int_0^T \left\{ \frac{\partial H}{\partial \mathbf{u}}\delta\mathbf{u}(t)\right\} dt \tag{7}$$

As we seek an open loop series of controls to minimise the dynamic cost J for constant conditions, $\delta\boldsymbol{x}(0) = \boldsymbol{0}$, the minimum cost must therefore exist where

$$\frac{\partial H}{\partial \mathbf{u}} = 0, \qquad \forall t \tag{8}$$

In [6] an approximation to the continuous solution is found using a discrete sequence of controls, each held constant for a small time step. Within the time period for each control, the cost gradient can then be identified as

$$\frac{\partial J}{\partial u_i} = \int_{t_{i-1}}^{t_i} \frac{\partial H}{\partial u_i}\,\mathrm{d}t \tag{9}$$

So it is feasible to establish a gradient based iteration optimisation of a sequence of discrete controls spanning the required time frame (Fig 1).

Note that, provided the control remains constant for its discretisation period, the method is valid irrespective of the duration. Also, independent controls can take different discretisations if required.

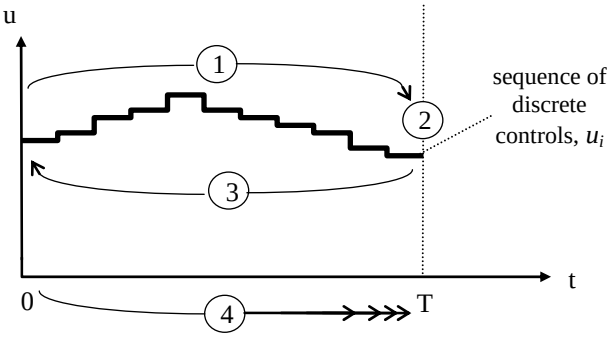

Fig. 1 Summary of GOC algorithm

(1) : Using the current discrete control sequence, integrate the state-space system from $\mathbf{x}(0)$ and evaluate $J_{[0,T]}$.

(2) : Evaluate the residual cost L_T and hence $\mathbf{p}(T)$ from Eqn. 6.

(3) : Integrate the costate system and $\partial H/\partial \boldsymbol{u}$ in reverse-time from the initial condition $\mathbf{p}(T)$. Calculate cost gradients from Eqn 9.

(4) : Update the control sequence by a line search optimisation along the steepest descent or successively conjugate gradients to minimise J (evaluated by repeating Stages 1 & 2).

3. VEHICLE MODEL

Allowing for active rear steer δ_r, the commonly used yaw / sideslip model is

$$\begin{aligned} \dot{u} &= \tfrac{1}{M}\left\{\sum f_{xi} - \sin(\delta_f)\left(f_{y1} + f_{y2}\right) - \sin(\delta_r)\left(f_{y3} + f_{y4}\right)\right\} \\ \dot{v} &= \tfrac{1}{M}\sum f_{yi} - ur \\ \dot{r} &= \tfrac{1}{I_{ZZ}}\left\{c\left(f_{x1} - f_{x2} + f_{x3} - f_{x4}\right) + a\left(f_{y1} + f_{y2}\right) - b\left(f_{y3} + f_{y4}\right)\right\} \end{aligned} \tag{10}$$

These make use of tyre forces f based on vertical loads Z which are determined using a 'stiff suspension' model which imposes equilibrium conditions on (unmodelled) roll, pitch and bounce degrees of freedom (see also [8]). Assuming a ratio λ between the front and rear suspension roll moments, the effect of both pitch and roll load transfer is accommodated via :

$$\begin{bmatrix} 1 & 1 & 1 & 1 \\ -a & -a & b & b \\ c & -c & c & -c \\ 1 & -1 & -\lambda & \lambda \end{bmatrix}\begin{bmatrix} Z_1 \\ Z_2 \\ Z_3 \\ Z_4 \end{bmatrix} = \begin{bmatrix} Mg \\ h\sum f_{xi} \\ h\sum f_{yi} \\ 0 \end{bmatrix} \tag{11}$$

The RWD driveline is simplified to simulate the four wheel speeds, assuming a nominal front drag torque and an active differential control input, u_x

$$\dot{w}_{1,2} = \tfrac{1}{I_w}\left\{-30 - r_r f_{x1,2}\right\} \tag{12}$$

$$\dot{w}_3 = \tfrac{1}{I_w}\left\{T_r(1-u_x) - r_r f_{x3}\right\}, \quad \dot{w}_4 = \tfrac{1}{I_w}\left\{T_r(1+u_x) - r_r f_{x4}\right\}$$

First order lag functions are then employed to simulate tyre force generation and impose a simple driver / vehicle bandwidth limitation on steer :

$$\begin{aligned} \dot{f}_{xi/yi} &= \rho_t \left(F_{xi/yi} - f_{xi/yi} \right) \\ \dot{\delta}_f &= \rho_\delta \left(\delta - \delta_f \right) \end{aligned} \tag{13}$$

Simulations are considered with various steer and drive torque inputs δ, T_r under the influence of controlled actuators δ_r and u_x, on a nominal, large vehicle parametrised as Table 1.

4. A NEW EXPONENTIAL TYRE MODEL

The GOC technique requires a smoothly analytic differentiable tyre model which delivers reasonably simple terms in the Jacobian. The simple form of Pacejka model has previously been used [8], but the derivative functions are very long, due in part to the use of functions of total slip, $k = \sqrt{S^2 + \alpha^2}$. Dugoff and Fiala models suffer similar problems.

A simple separated form $F_y = f_1(S, \alpha, Z)$, $F_x = f_2(S, \alpha, Z)$ would be beneficial for GOC and is likely to have applications elsewhere (in Extended Kalman filters for example). If we consider the fundamental shape of tyre force curves, having a distinctive peak in some regions, a smooth exponential rise in other regions, and settling to a constant force at extreme slip values, an appropriate basis function is (eg for lateral force),

$$F_y = Z\left(A\alpha e^{-b\alpha} + B\left(1 - e^{-b\alpha}\right)\right)\mathrm{sgn}(\alpha) \tag{14}$$

where the relative magnitudes of parameters *A* and *b* determine the existence or not of a distinct peak, the second term delivers the constant force at extremes, and interestingly, little loss of accuracy results from both exponentials having the same decay constant, *b*. Of course the three parameters *A*, *B* and *b* vary with the opposite slip angle (the function is symmetrical for F_x) and vertical load.

The full model was identified by fitting to forces generated from the simple Pacejka similarity model for a dry tarmac road, as described in [8]. *A*, *B* and *b* were optimised using a Nelder-mead algorithm for F_y against α, across the full range of *S* and *Z*. Candidate functions to explain the variations in each parameter with *S* and *Z* were then identified using engineering judgement; the parameters for these functions were then optimised as before, to find the full parameter set. After repeating the optimisation to find new parameters on the symmetric model for F_x the result is

$$\begin{aligned} A_x &= p_{x0} e^{-p_{x1} Z'} e^{-p_{x2}\alpha} + p_{x3}\alpha \\ B_x &= \left(p_{x4} - p_{x5} Z'\right)\left(p_{x6} - p_{x7}\alpha\right) \\ b_x &= p_{x8} e^{-p_{x9}\alpha} \\ F_x &= Z\left(A_x S e^{-b_x S} + B_x\left(1 - e^{-b_x S}\right)\right)\mathrm{sgn}(S) \end{aligned} \tag{15}$$

$$\begin{aligned} A_y &= p_{y0} e^{-p_{y1} Z'} e^{-p_{y2} S} + p_{y3} S \\ B_y &= \left(p_{y4} - p_{y5} Z'\right)\left(p_{y6} - p_{y7} S\right) \\ b_y &= p_{y8} e^{-p_{y9} S} \\ F_y &= Z\left(A_y \alpha e^{-b_y \alpha} + B_y\left(1 - e^{-b_y \alpha}\right)\right)\mathrm{sgn}(\alpha) \end{aligned} \tag{16}$$

where $Z' = Z/1000$.

Thus force in each direction depends on 10 non-physical parameters (given in Table 1) and though the force calculations are conducted independently (making Jacobian functions more straightforward) the resulting pair of forces obey expected combined slip dependencies (eg friction ellipse). Fig. 2 shows that the new model behaves as expected, and although the fit to the original model is not perfect, the original is itself simplified, so optimisations to raw tyre test data will be needed to more closely determine accuracy. Vehicle simulation results, and the results of control optimisation in this paper show the model to be appropriate, if, at present, nominal.

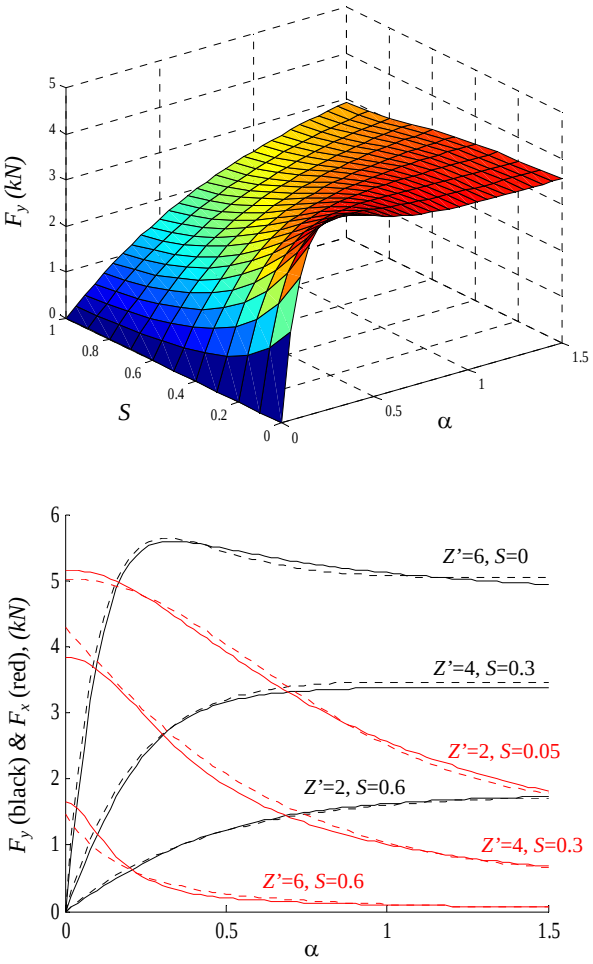

Fig. 2 New tyre model (top), and (bottom, dashed) compared with simple Pacejka model (solid) as a function of vertical load Z', lateral slip α and longitudinal slip, *S*

5. YAW RATE TARGET SETTING

A very common approach in chassis control (eg [3-5]) and one which allows easy assessment of performance is employment of a reference model or target yaw rate. A number of papers suggest linear reference conditions, [4,5] and some reduce this further, setting yaw rate demand according to the steady-state yaw rate gain function for a prescribed linear understeer gradient K;

$$r_{dem} = \frac{u\delta}{L + \left(Ku^2/g\right)} \tag{17}$$

Fig. 3 compares steady-state acceleration response of the test vehicle with this linear reference, showing potential problems for continuous control; if the linear model is tracked perfectly, as we reach the limit of adhesion the actuator demand will presumably increase unfeasibly, and also the driver will not feel the limit approaching. A nonlinear alternative is also illustrated, which lowers understeer at low lateral accelerations, but saturates more progressively near the limit. The proposed model,

$$\delta = \frac{rL}{u} + \frac{kr}{a_p - ur} \tag{18}$$

can be rearranged to give the correctly signed yaw rate demand function :

$$r_{dem} = \frac{\delta}{2Lu|\delta|}\left\{La_p + ku + \delta u^2 - \sqrt{\left(La_p + ku + \delta u^2\right)^2 - 4La_p\delta u^2}\right\} \tag{19}$$

If the steer angle is first filtered through a suitably parametrised 2nd order transfer function, this yaw rate demand is similar to a nonlinear reference bicycle model, having sensible saturation behaviour, but with constant transient response across vehicle speed and acceleration. This may not represent a perfect response for the driver, but is expected to be preferable to a reference model with simply saturating axle forces, and can readily be tuned in development.

Table 1 summarises all the required model, tyre and target setting parameters.

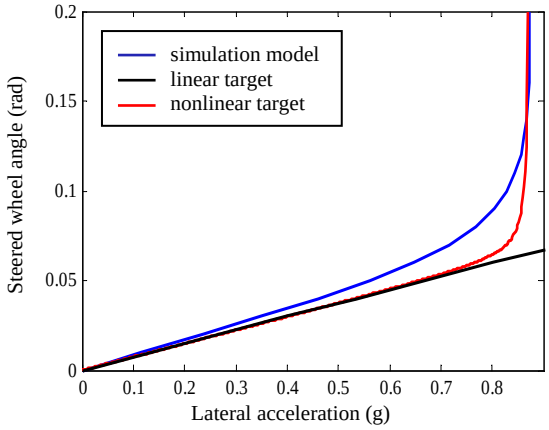

Fig 3 : Vehicle and proposed target steady-state response

Table 1 Model Parameter Nomenclature and Settings

parameters *(values)*	
M	mass (*1900 kg*)
I_{zz}	yaw moment of inertia (*4200 kgm*^{2})
I_w	wheel and driveline inertia (10 *kgm*^{2})
a	longitudinal Distance of C of G to front axle (*1.16 m*)
b	longitudinal Distance of C of G to rear axle (*1.54 m*)
c	half track (0.75 *m*)
h	C of G height above roll axis (*0.5 m*)
λ	roll moment distribution factor (*1.5*)
r_r	wheel rolling radius (*0.3 m*)
ρ_t	tyre lag coefficient (*100 rad/s*)
ρ_δ	steering lag coefficient (*30 rad/s*)
K	understeer for linear yaw rate demand (0.1 °/g)
k	nonlinear yaw rate demand coefficient (*0.01*)
a_p	peak accel for nonlinear yaw rate demand (*8.43 m/s*^{2})
ω_n	2nd order lag for nonlinear yaw rate demand (*10 rad/s*)
ζ	2nd order lag for nonlinear yaw rate demand (*0.9*)
p_{x0}, $p_{x1..}$	longitudinal tyre force coefficients (*14.9485 0.0675 7.7883 0.2067 0.4201 0.0104 2.2250 0.0974 8.0495 2.0585*)
p_{y0}, $p_{y1..}$	lateral tyre force coefficients (*10.6987 0.1229 6.5080 0.3915 0.8062 0.0207 1.2293 0.1349 6.4961 2.1093*)

6. SIMULATION EXPERIMENTS

GOC is used to optimise the rear steer δ_r, and the idealised differential ratio u_x, using the cost function

$$J = \int 100\left(r - r_{dem}\right)^2 + \delta_r{}^2 + \gamma v^2 dt \tag{20}$$

with γ = 0.01 or γ = 0 used to examine the value of lateral velocity regulation. Note that no cost is attributed to u_x. An interesting comparison can be made with a simple, nominally tuned PID control, actuating rear steer only as a function of yaw rate error (r - r_{dem}), according to

$$G_c(s) = \frac{2\left(s^2 + 75s + 10\right)}{\left(s^2 + 100s\right)} \tag{21}$$

Steady-state response of the controllers is examined in Fig. 4, where steer δ is ramped to +15° over 50s while forward speed is maintained at 20m/s with a small ramped input to T_r. (γ = 0.01).

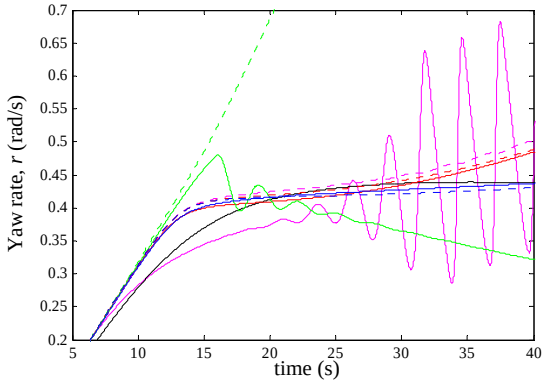

Fig 4(a) : Steady-state ramp steer response, showing yaw rate (solid) and yaw rate demand (dashed)

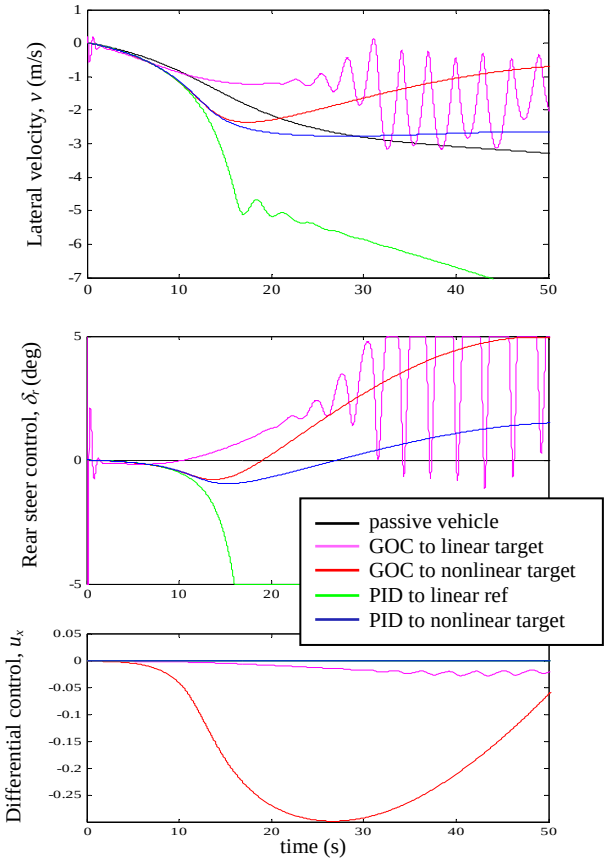

Fig 4 : Steady-state ramp steer response

The linear yaw rate reference fails for both PID and GOC as we approach the limit of lateral acceleration. GOC maintains a feasible yaw rate demand but with increasingly oscillatory control around the tyre adhesion peak. Without the applied 5° limit on δ_r the PID controller becomes unstable even sooner, and although this negative rear steer seems an undesirable, unstable control, it does meet the low lateral acceleration requirement for understeer reduction. Most significant is the success of the PID control when the nonlinear target yaw rate is employed, which suggests that simple control can be effective provided a sensible reference is used. GOC uses quite a lot more actuation, in 2 channels, to achieve little more than a modest reduction in lateral velocity.

Continuing with the feasible nonlinear yaw rate reference, transient behaviour is examined with a 3° step steer at a steady forward speed u = 30m/s (maintained using a constant T_r = 100Nm) in Fig. 5.

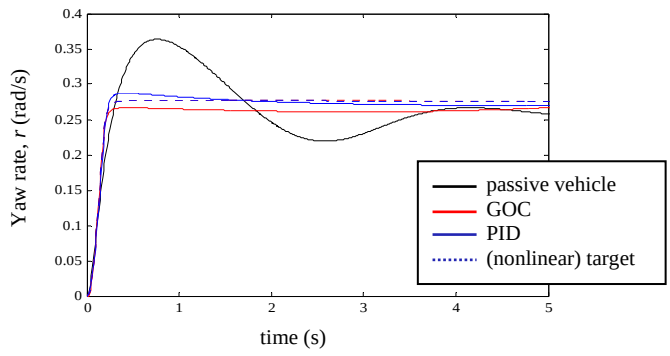

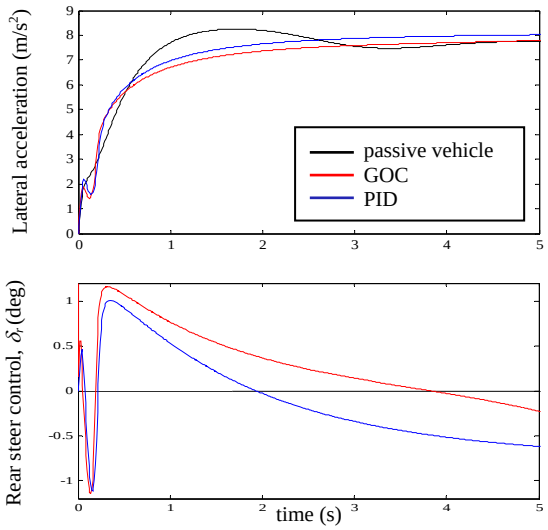

Fig 5 : Step-steer response

Both controllers show the improved relative stability afforded by close tracking of yaw rate demand, again with PID as effective as GOC. A slight improvement in lateral velocity occurs for GOC, coming from a small u_x peaking at -0.06, not shown. Costs for GOC / PID are J = 0.62 / 0.74 compared with the passive case, J = 1.62. Lateral acceleration also initially rises more quickly than the uncontrolled case, but the subsequent rise from 6–8m/s^2 is slowed by the increasing negative vehicle lateral velocity as rear steer reduces. It is not clear what implication, if any, this might have from a driveability perspective.

Further confirmation of effective transient control can be seen in Fig. 6, which shows the response to a double lane-change manoeuvre taken at 35m/s. The uneven yaw rate response of the passive case is controlled well by GOC, and adequately by PID. A note of caution is seen in the very similarly controlled lateral acceleration plots however, where the rear steer oscillations (around 4° in magnitude but peaking briefly at 10°, not shown) cause undesirable variability. This is almost certainly due to the arbitrary 2nd order delay in the yaw reference function, which would undoubtedly need to vary with forward speed in a practicable controller. The delay in δ_r between GOC and PID seen in Fig. 5 and more clearly in Fig. 6 results from the non-causal nature of the optimisation of controls for GOC; it is interesting that in spite of the fully nonlinear optimisation this seems to be the only significant difference between the two, and it results in very little in the way of PID performance degradation.

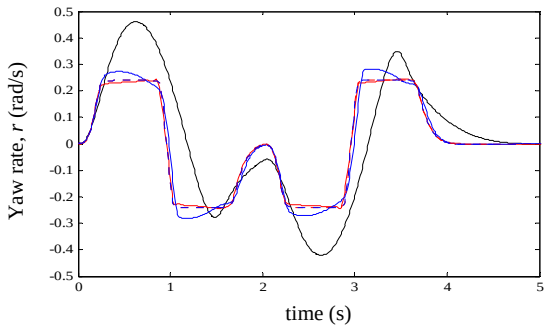

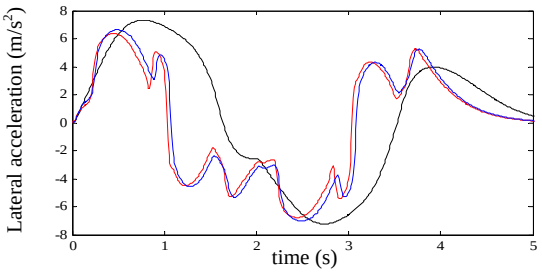

Fig 6 : Response to a high speed lane change

The suggested PID control is not a universal solution however, as Fig. 7 shows. Here the (RWD) vehicle is accelerated from 5m/s, at 4m/s^2 with a steer angle of 5° simultaneously applied. With the high torque (T_r = 1500Nm) the passive vehicle loses traction at the rear, and spins, and the PID would require an unfeasibly large (and incorrectly modelled) rear steer to regain a level of control. GOC demonstrates how, with significant control input to δ_r and u_x, it is possible to stay close to the yaw reference. It also maintains low lateral velocity, regardless of the setting of γ. The control sequence is complex and oscillatory however, as it fights the saturations in lateral force at the rear; it may not easily be emulated by any simple alternative controller.

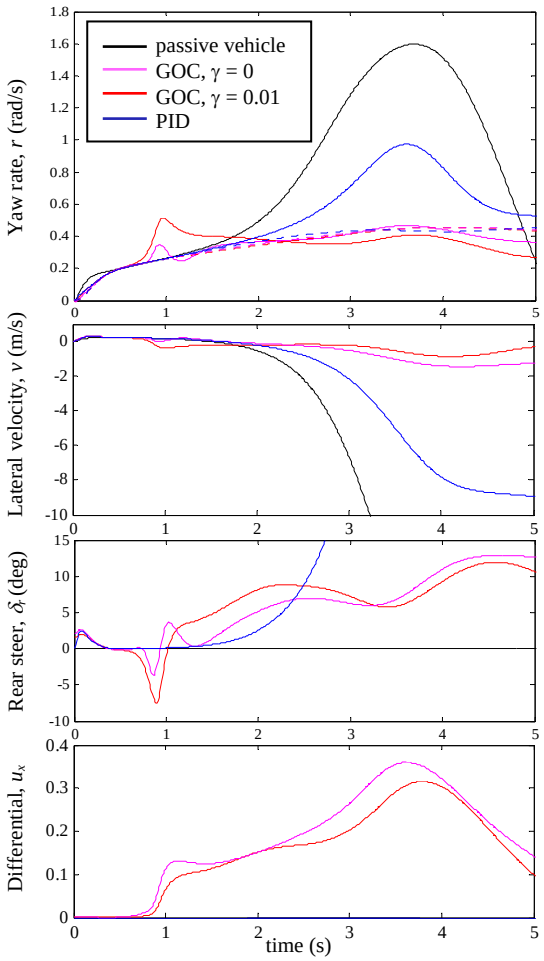

Fig 7 : Response to destabilising input; steer under hard acceleration

7. CONCLUDING REMARKS

In the stable range of vehicle handling, provided a suitably realistic yaw rate target is employed, the simple single channel PID control performs almost identically to the best possible nonlinear optimal reference. The results also suggest that lateral velocity minimisation may be unnecessary. We might therefore assume that a very simple control structure is effective for all constant speed scenarios.

When destabilisation is triggered using hard acceleration, the simple controller is no longer effective (if sensible assumptions are made regarding actuation limits). Also, for this test the two channel sequence of nonlinear optimal controls is complex and convoluted, which suggests simple linear state feedback control may not be applicable. Note however that in this paper the control sequence was derived with full a-priori knowledge of the manoeuvre. It is possible to reconfigure the GOC to deliver the optimal *causal* control sequence; future research will thus reconsider destabilising scenarios using a causal GOC sequence, with a view to identifying a nonlinear feedback function of measurable states. Practical application should then be viable, provided the vehicle and tyre models are identified from a suitable test vehicle, and some compensation can be applied for varying surface friction conditions.

REFERENCES

[1] van Zanten, A. T., “Bosch ESP Systems: 5 Years of Experience,” SAE paper 2000-01-1633, 2000

[2] Park, K., Heo, S-J. et al, “Development of Integrated Chassis Control Algorithms to Improve Vehicle Dynamics,” Proceedings of the 8th International Symposium on Advanced Vehicle Control (AVEC), Taipei, Taiwan, August 2006, pp 883-888

[3] Marino, R., Scalzi S., and Cinili, F., “Nonlinear PI Front and Rear Steering Control in Four Wheel Steering Vehicles,” Vehicle System Dynamics, Vol 45, No 12, 2007, pp 1149-1168

[4] Chen, H-H., and Chandy, A., “Active Handling Enhancement for Chassis Control Systems,” International Journal of Vehicle Autonomous Systems, Vol 5, No 1-2, 2007, pp 79-94

[5] Cheong, J., Eom, W. and Lee, J., “Cornering Stability Improvement for 4 Wheel Drive Hybrid Electric Vehicle,” IEEE International Symposium on Industrial Electronics, 2009, pp853-858

[6] Gordon, T.J., and Best, M.C., “On the Synthesis of Driver Inputs for the Simulation of Closed-loop Handling Manoeuvres,” International Journal of Vehicle Design, Vol 40, No 1/2/3, 2007, pp 52-76

[7] Bryson, A.E. and Ho, Y.C., “Applied Optimal Control: Optimisation, Estimation and Control,” *Hemisphere*, New York, 1975

[8] Gordon, T.J. and Best, M.C., "A Sequential Dual Model Approach to Lap Optimisation" , Proceedings of the 6th International Symposium on Advanced Vehicle Control (AVEC), Hiroshima, Japan, September 2002, pp 99-104